JOURNAL OF AGRICULTURAL AND FOOD CHEMISTRY

pubs.acs.org/JAFC Article

Comparative Proteomic Analysis Reveals Candidate Pathways Related to the Effect of Different Light Qualities on the Development of Mycelium and Fruiting Body of *Pleurotus ostreatus*

Liping Zhu,[#] Yao Su,[#] Shunan Ma, Lizhong Guo, Song Yang,[*] and Hao Yu[*]

Cite This: *J. Agric. Food Chem.* 2024, 72, 1361−1375 Read Online

ACCESS | Metrics & More | Article Recommendations | Supporting Information

ABSTRACT: Light affects the morphology and physiology of *Pleurotus ostreatus*. However, the underlying molecular mechanism of this effect remains unclear. In this study, a label-free comparative proteomic analysis was conducted to investigate the global protein expression profile of the mycelia and fruiting bodies of *P. ostreatus* PH11 growing under four different light quality treatments. Among all the 2234 *P. ostreatus* proteins, 1349 were quantifiable under all tested conditions. A total of 1100 differentially expressed proteins were identified by comparing the light group data with those of the darkness group. GO and KEGG enrichment analyses indicated that the oxidative phosphorylation, proteasome, and mRNA surveillance pathways were the most related pathways under the light condition. qRT-PCR verified that the expression of the white collar 1 protein was significantly enhanced under white light. Additionally, glutamine synthetase and aldehyde dehydrogenase played important roles during light exposure. This study provides valuable insight into the *P. ostreatus* light response mechanism, which will lay the foundation for improved cultivation.

KEYWORDS: *Pleurotus ostreatus, oxidative phosphorylation, proteasome, mRNA surveillance, glutamine synthetase*

INTRODUCTION

Environmental factors such as nutrients, temperature, carbon dioxide concentration, and light are crucial for the growth of mushroom-forming fungi.[1−3] Specifically, light plays a significant role in regulating the growth, development, and metabolism of mushrooms as an environment signal, and factors such as light intensity and wavelength are particularly important.[4−8] Therefore, providing proper light conditions is essential for the induction and development of fruiting bodies. The effect of light has been investigated in various mushrooms, including *Coprinopsis cinerea*,[9] *Inonotus rheades*,[10] *Lentinula edodes*,[11−15] *Pleurotus ostreatus*,[16,17] *Pleurotus eryngii*,[18−20] *Cerrena unicolor*,[21−23] and *Hypsizygus marmoreus*.[24,25] Studies have shown that different light qualities have varying effects on the growth of mycelium and the development of primordia or fruiting bodies.[26] For example, although most mushrooms do not require light during the mycelial growth stage, the mycelia of *Cordyceps militaris* exposed to white light exhibit significantly faster growth compared to those kept in the dark. In contrast, blue light significantly inhibits the mycelial growth in *C. militaris* and leads to a notable reduction in biomass.[27] Previous studies have indicated that ultraviolet and blue light are effective wavelengths for inducing fruiting bodies.[1] Specifically, blue light produces fruiting bodies with superior characteristics compared to other wavelengths, making it a commonly used light source to cultivate *L. edodes*[15] and *H. marmoreus*.[24,25] However, white light is generally used for most mushrooms, including oyster mushrooms, considering its effectiveness and convenience.

Pleurotus ostreatus is a type of oyster mushroom and the second most cultivated and consumed editable mushroom worldwide. *P. ostreatus* is known for its pleasant taste and high medicinal value.[16,28] Oyster mushroom species and varieties require a specific light intensity to generate properly formed fruiting bodies.[29] Light is not essential for mycelial growth but is a decisive factor (length/intensity) for a high yield with good quality during the initiation and growth of fruiting bodies.[29] It has been previously demonstrated that blue light inhibits the growth of oyster mushroom mycelia[30,31] but enhances the growth and development of *P. ostreatus* fruiting bodies after differentiation of the primordium.[16] However, limited information is available regarding the effects of light on the development of fruiting bodies in *P. ostreatus*. Moreover, studies have indicated that light not only affects visual quality but also has an impact on the ingredients.[29] Although the effects of light wavelengths on mycelia growth or primordial differentiation of oyster mushrooms have been individually investigated using transcriptome technology,[13,18−20] the proteomic analysis method has not been applied. Specifically, proteomic analysis has been successfully applied in a few studies of *P. ostreatus*, including investigations of factors, such as CO_2 concentration, primordial differentiation, and heat stress.[32−35] Therefore, it is necessary to conduct proteomic analysis on the mycelia and fruiting bodies of *P. ostreatus*.

In this study, we conducted a comparative proteomic analysis of *P. ostreatus* in the early mycelial growth stage and fruiting body stage cultivated under four different light conditions,

Received: August 29, 2023
Revised: November 14, 2023
Accepted: December 15, 2023
Published: January 3, 2024

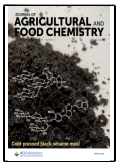

namely, white light, red light, blue light, and darkness. GO and KEGG enrichment analyses were performed to describe the *P. ostreatus* regulatory pathway. Our objective is to present a comprehensive data set exploring changes in protein expression profiles within fungal cells in response to variable light qualities. This research will contribute to a better understanding of *P. ostreatus* photobiology as well as the light-dependent metabolism and behavior of this commercially important species. The findings will aid in optimizing cultivation practices and allowing for higher *P. ostreatus* yield and quality.

MATERIALS AND METHODS

Strains, Cultivation Conditions, and Sample Collection. The *P. ostreatus* strain PH11 utilized in this study was obtained from the Center of Mushroom Culture Conditions (NCMCC, mushroom-seed.cn) with deposition number NCMCCNO 230011. The mycelia were cultured and subcultured in potato dextrose agar (PDA) medium at 25 °C. For subsequent experiments, mycelial plugs with a diameter of 5 mm (about 8 days) were cut from the margin of seed agar cultures and placed at the center of new PDA plates (90 mm) covered with cellophane. These plates were transferred into light-tight boxes (40 × 30 × 30 cm), each providing a different light quality: white light (400−700 nm, W group), red light (620−760 nm, R group), blue light (492−572 nm, B group), and darkness (D group), respectively. The plates in each box were initially incubated at 25 °C for 10 days without light and then subjected to their respective light conditions for 48 h. Six plates were prepared for each condition, and mycelia from three selected plates with a similar growth condition were scraped from the plates as biological replicates. The mycelia in one sample were from one plate. Then, the mycelia were snap-frozen in liquid nitrogen and stored at −80 °C for subsequent protein extraction. Furthermore, the fruiting bodies of *P. ostreatus* PH11 were cultured in cultivation bags filled with a previously described cultivation substrate (400 g).[34] After sterilization at 121 °C for 2 h and cooling at room temperature in an aseptic environment, the cultivation bags were inoculated with 2% *P. ostreatus* liquid spawn in PDB medium and incubated at 25 °C in a dark culture room until the medium was entirely covered with mycelia and the primordium had formed. The cultivation bags were transferred to a climate chamber set to a constant 20 °C and humidity of 95% to produce fruiting bodies. The length of the mushroom bud was measured daily until it reached 3 cm. Then, the mushrooms were treated with different light conditions, including white light, blue light, red light, or darkness (as a control), respectively. Fruiting body samples were collected after 6 days of light exposure (24 h/day), frozen in liquid nitrogen, and stored at −80 °C for further analysis. Six cultivation bags were prepared for each condition, and the fruiting bodies from four bags for each condition were selected as biological replicates for each group. Two fruiting bodies from each bag were mixed as a sample for further proteomic analysis.

Protein Extraction and Peptide Digestion. Protein was extracted from frozen *P. ostreatus* PH11 samples using a method described previously.[36] Briefly, 100 mg of the frozen sample (either mycelia or fruiting bodies) was placed in a tube and lysed using a JXFSTPRP-24 Tissuelyser (Jingxin, Shanghai, China) at a frequency of 150 Hz for 60 s. Subsequently, 1 mL of UDT buffer (8 M urea, 0.1 M DTT, and 0.1 M Tris−HCl pH 8.5) supplemented with Halt Protease Inhibitor Cocktail (Thermo Fisher, Shanghai, China) was added to the centrifugation tube. After vortexing for 5 min, ultrasonication was performed for 30 min (6 s on, 15 s off) to disrupt the DNA. The tissue debris was eliminated by centrifugation at 12,000 × g for 10 min at 4 °C, and the supernatant was transferred to a new tube. The protein concentration was determined using the Bradford method. Thereafter, enzymolysis was conducted using the FASP method, as described previously.[37] Initially, the protein sample (100 μg) was dissolved in 300 μL of UA buffer to eliminate low-molecular-weight impurities after centrifugation. The samples were alkylated with 50 mM iodoacetamide for 30 min at room temperature in the absence of light. 2 μg of modified trypsin (Promega, Madison, Wisconsin, USA) was used for enzymolysis, and digestion was carried out with gentle shaking at 37 °C for 12 h. The resulting peptides were eluted using 50 mM NH_4HCO_3 and desalted on a C18 SPE column (66883-U; Merck, Darmstadt, Germany), following Rappsilber et al.[38] Subsequently, the desalted peptide sample was lyophilized in an RVC 2-25 CD plus vacuum concentrator (Christ, Osterode am Harz, Germany).

Label-Free LC-MS/MS Quantitative Proteomics Analysis. The peptides were resuspended in 0.1% formic acid, and their concentration was adjusted to 0.6 μg/μL with a NanoDrop One spectrophotometer (Thermo Fisher Scientific Inc.). Liquid chromatography−mass spectrometry analysis was performed using the Nano-LC system coupled with the Orbitrap Fusion Tribrid (Thermo Fisher Scientific, San Jose, California, USA). The MS instrument was operated in data-dependent acquisition mode, and full MS scans were performed across a mass range of m/z 350−1500 with detection in the Orbitrap (resolution of 120 K) and an auto gain control setting of 100,000. The resolution for MS1 was 60 K, and the resolution for MS2 was 15 K. The filter charge states were set to 2−7. To improve utilization of the mass spectrum, the automatic gain control was 2E5, the maximum injection time was 35 ms, and the dynamic exclusion time for the tandem MS scan was 60 s to avoid repeated scanning of the parent ions. Various chromatographic gradient lengths from 60 to 240 min were tested to separate the peptides. Elution of all gradients started with 5% (v/v) acetonitrile (ACN) (0.1% formic acid), which was ramped up to 32% (v/v) ACN (0.1% formic acid). Three biological replicates were used for each group, and each sample was subjected to two technical replicates.

Identification and Quantitation of Proteins. The raw data were analyzed using MaxQuant 2.0.2.0 against the *P. ostreatus* PC15 proteome database from the UniProt proteome database (Proteome ID: UP000076154, accessed on 15 February 2023) with default parameters. Identifying the proteins required the presence of at least one peptide with a false discovery rate <0.01 for PSM and protein identification. The initial maximum precursor mass tolerances were 20 ppm for the first search and 4.5 ppm for the main search.

Bioinformatics Analysis. The original data from MaxQuant were normalized using the median normalization method (with the same median value), and then the missing values of a protein with at least two valid data were filled using the KNN (5) imputation strategy.[39] The standard for differentially expressed proteins (DEPs) was a p-value <0.05. The heatmaps and Venn diagrams were analyzed with the R-ggcyto 1.24.0 tool.[40] The Gene Ontology (GO)[41] (http://geneontology.org/ (accessed on 10 March 2023)) and Kyoto Encyclopedia of Genes and Genomes (KEGG)[42] (http://www.kegg.jp/ (accessed on 15 March 2023)) databases were utilized to analyze the functional annotations and metabolic pathways of the DEPs. The number of DEPs assigned to each category was tallied, and the significance of the enrichment was calculated by using the hypergeometric distribution test. Enrichment diagrams of the GO/KEGG pathway annotations were generated using the OmicShare online tools (https://www.OmicShare.com/tools).

Enzyme Assay. After light treatment, partial of the fruiting bodies were also collected for the determination of soluble protein content. Briefly, 0.25 g of the fruiting body sample was added into 5 mL of distilled water and vigorously shaken to ensure thorough mixing. The mixture was then centrifuged at 12,000 rpm for 12 min, and the supernatant was collected. Next, 0.2 mL of the supernatant was thoroughly mixed with 5 mL of Coomassie Brilliant Blue G-250 staining solution and left to stand for 5 min, and the OD595 nm was measured. The laccase and manganese peroxidase (MnP) activities were measured according to the method described before using crude enzyme extract.[43] The crude extract was generated as follows: 8 g of culture medium from the same region of the fungal bag was collected and mixed with 32 mL of 1× phosphate-buffered saline (PBS). The mixture was shaken at 125 rpm at 25 °C for 30 min and subsequently centrifuged at 6000 g for 10 min to obtain the supernatant.

Validation of the Proteomic Data by Quantitative Real-Time Polymerase Chain Reaction (qRT-PCR). A set of 22 proteins displaying significantly differential expression in response to the different light qualities in the enriched KEGG metabolic pathways

https://doi.org/10.1021/acs.jafc.3c06083
J. Agric. Food Chem. 2024, 72, 1361−1375

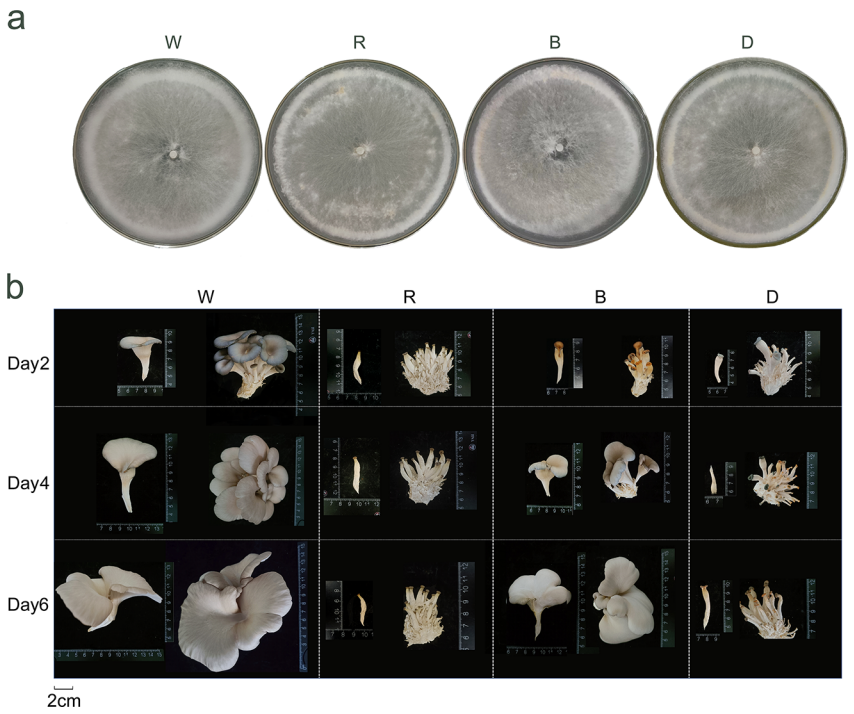

Figure 1. Morphological comparison of *P. ostreatus* PH11 under different light qualities. (a) Morphology of mycelium under different light treatments. (b) Morphological changes of fruiting bodies under different light treatments at the day 2, 4, and 6. W, white light; R, red light, B, blue light; D, darkness.

were carefully chosen for qRT-PCR validation. Total RNA was extracted from the mycelium/fruiting body samples using an RNA reagent kit (Omega, Norcross, Georgia, USA). Subsequently, the RNA samples were treated with RNase-free DNase I (Omega) to eliminate residual genomic DNA. The resulting cDNA was used as the template, which was synthesized according to the manufacturer's protocol for the PrimeScript RT Reagent Kit (Vazyme, Nanjing, China). The specifically designed qRT-PCR primers of these 22 DAPs are presented in Supplementary Table S1. To ensure accurate normalization, the genes encoding glyceraldehyde-3-phosphate dehydrogenase (A0A067NKG0) were selected as internal controls. All samples were subjected to three biological replicates, and the relative gene expression levels were calculated by using the $2^{-\Delta\Delta Ct}$ method.

Data Availability. The raw data for the proteomic analysis reported in this paper have been deposited in the OMIX, China National Center for Bioinformation/Beijing Institute of Genomics, Chinese Academy of Sciences (https://ngdc.cncb.ac.cn/omix: accession no. OMIX004627).

RESULTS

***P. ostreatus* Phenotypes under the Different Light Treatments.** After 48 h of light exposure, significant differences in the growth and morphology of the mycelia were observed under different light treatments (Figure 1a). Colonies with thick and dense mycelial strands were observed under white and blue light. In contrast, the mycelia were much thinner under darkness and red light, with the thinnest mycelia appearing under red light. Additionally, the mycelia at the edges clustered with clear bondage under blue and red light, indicating that blue/red light inhibits mycelial growth. Evident aerial mycelia formed under white light and darkness, while the mycelia clustered under red light and darkness. These results suggest that *P. ostreatu* mycelia thrived under white light, while red light and darkness facilitated differentiation. It has been reported that blue light suppresses the growth of oyster mushroom mycelia[30] but that it is important for inducing primordium differentiation and fruiting body development in *P. ostreatus*.[16] As mentioned above, white and blue light significantly promoted the growth of *P. ostreatus* fruiting bodies while red light and darkness significantly inhibited them (Figure 1b). This observation indicates that light quality plays a crucial role in the formation and growth of fruiting bodies. The characteristics of the fruiting body were also measured (Figure S1). Measuring the weight of the individual fruiting bodies, corresponding to the yield of mushrooms, revealed that the heaviest fruiting body appeared under white light and the lightest was observed under red light (Figure S1a). The diameter ratio of the cap and stipe, which is an important parameter for market appearance, showed a much higher diameter ratio under white light and blue light and a significantly lower ratio under red light and darkness (Figure S1a). This suggested that white and blue light effectively promoted the growth of *P. ostreatus*. This conclusion aligns with the findings for most *Pleurotus* species but contradicts the results of studies on *P. eryngii*, *C. militaris*, and *Flammulina velutipes*,[26,27,44] where red light significantly enhanced growth. This result demonstrates the diversity of the light effect on different mushrooms. Additionally, the activities of laccase were significantly higher under white and blue light than under red light and darkness (Figure S1b). However, MnP activity was lower under all light conditions compared with that in darkness and blue light displayed the least activity (Figure S1b). The highest soluble protein content was detected under white light (Figure S1b). These results indicate that fruiting body metabolism is promoted under white light stimulation.

Proteome Profile of *P. ostreatus* Samples During Growth under Various Light Qualities and Correlations between the Samples. The mycelia samples of *P. ostreatus* strain PH11 prepared from the different light conditions were classified into four groups, namely, the white light group (MycW), the red light group (MycR), the blue light group

https://doi.org/10.1021/acs.jafc.3c06083
J. Agric. Food Chem. 2024, 72, 1361−1375

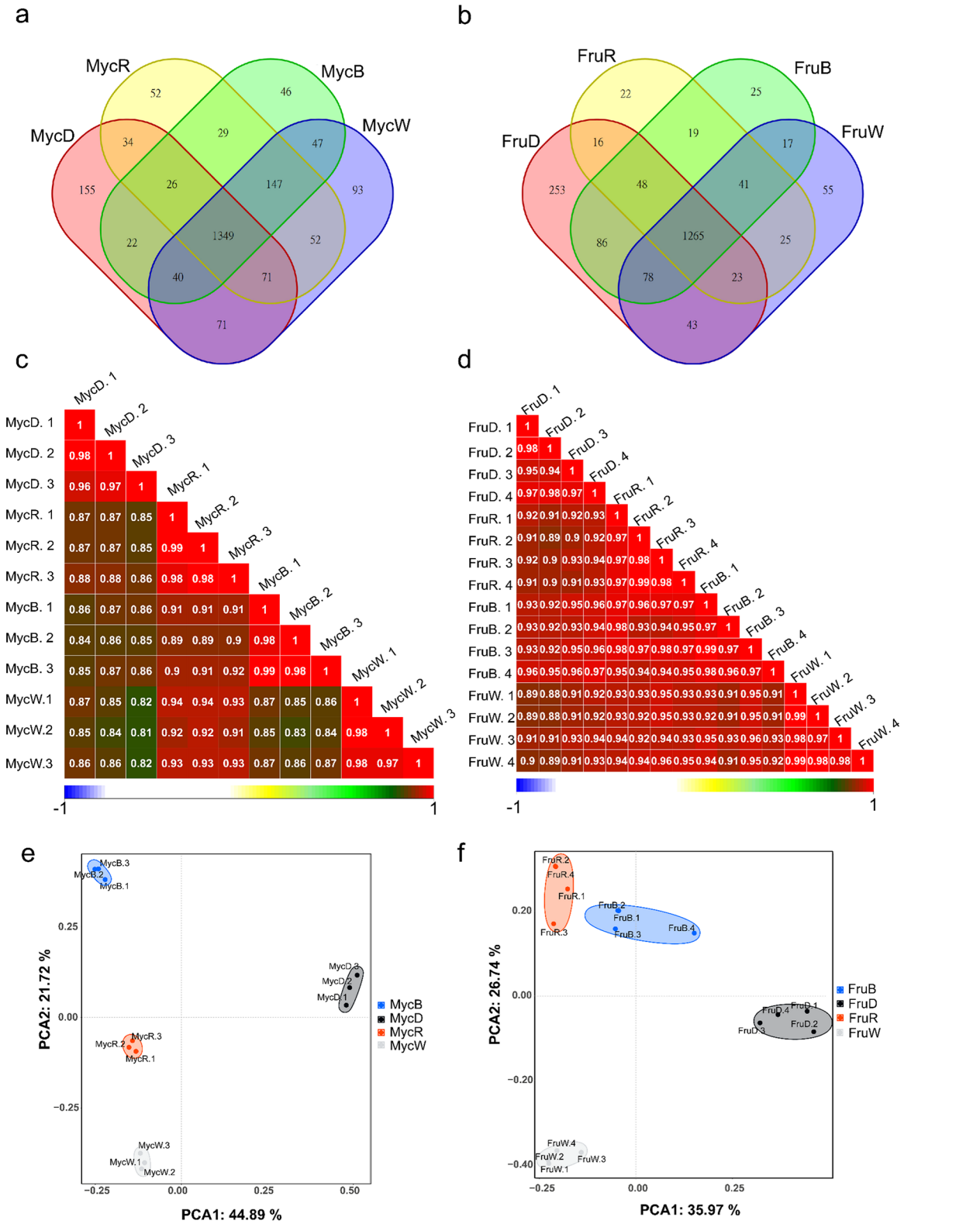

Figure 2. Proteomics statistics of the proteome data of *P. ostreatus* samples under different light conditions. (a) and (b) Venn diagram demonstrating the number of expressed proteins obtained from the mycelium and fruiting body samples, respectively. (c, d) PCC analysis and PCA for proteome data of mycelium samples. (e, f) PCC analysis and PCA for proteome data of fruiting body samples. Myc, mycelium; Fru, fruiting body; W, white light; R, red light; B, blue light; and D, darkness.

(MycB), and the darkness group (MycD) as the control. Similarly, the fruiting body samples of *P. ostreatus* strain PH11 were classified into four groups, FruW, FruR, FruB, and FruD, accordingly.

A total of 2234 quantifiable proteins were identified in the mycelial proteome, among which 1349 shared proteins were shared among all groups (Figure 2a). A total of 2016 quantifiable proteins were identified in the fruiting body, and 1265 shared

https://doi.org/10.1021/acs.jafc.3c06083
J. Agric. Food Chem. 2024, 72, 1361−1375

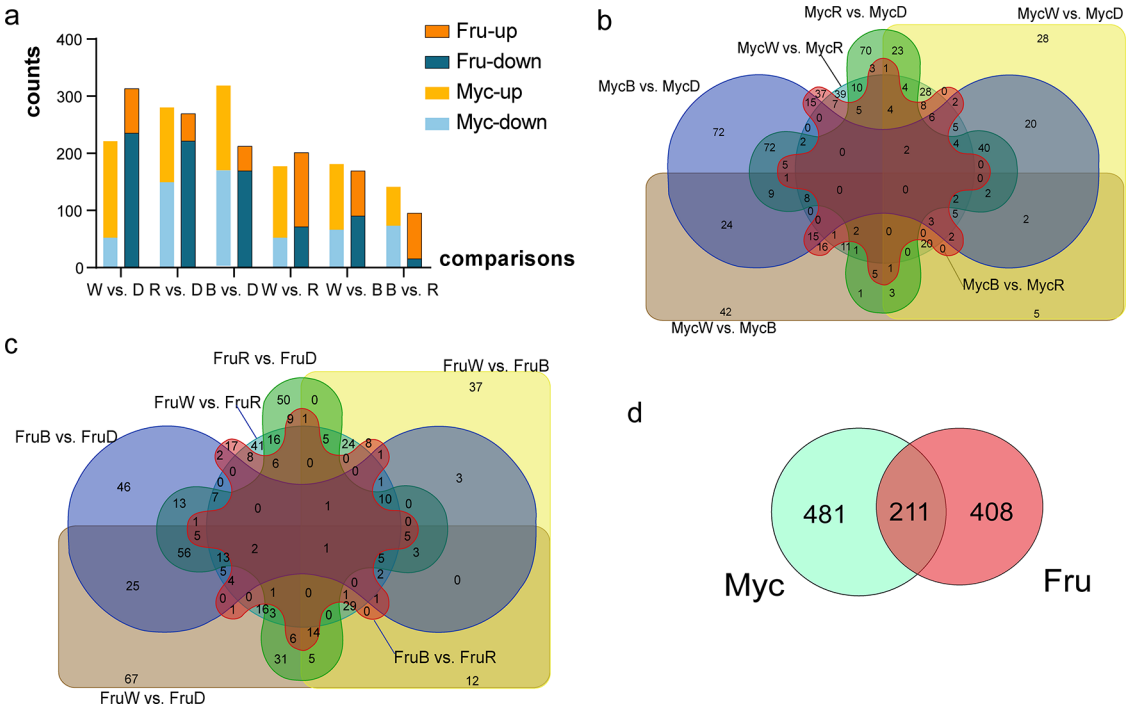

Figure 3. Analysis of DEPs of each comparison group between different light conditions. (a) Statistics of the upregulated and downregulated DEP profiles of the mycelium/fruiting body samples in six comparisons, W vs D, R vs D, B vs D, W vs R, W vs B, and B vs R. up, upregulated; down, downregulated; Myc, mycelium; Fru, fruiting body. (b) and (c) Venn diagrams of the intersection and the number of all nonredundant DEPs among six comparisons from the mycelium sample and fruiting body sample, respectively. (d) Venn diagram of the number of shared and unique DEPs among the mycelium sample and fruiting body sample.

proteins were identified among the groups (Figure 2b). A total of 155/253 proteins were individually expressed under the darkness condition, and 147/41 shared proteins were identified in all groups except the darkness group, referring to the mycelial samples/fruiting body samples (Figure 2a,b), which would be analyzed subsequently. Heat maps based on Pearson's correlation coefficient (PCC) between the light groups showed high intragroup correlations and low intergroup correlations with large differences (Figure 2c,d). The MycD group was moderately correlated (0.84−0.87) with all of the light groups (MycW, MycR, and MycB) (Figure 2c). The FruR and FruW groups demonstrated slightly more noticeable differences compared to those of the FruD group (Figure 2d). Principal component analysis (PCA) showed that light quality was responsible for 44.89% of the variance at the PCA1 level for the mycelial groups and 35.97% for the fruiting body groups. Dispersion at the PCA2 level was observed between MycW and MycB (Figure 2e), as well as between FruR and FruW (Figure 2f). Notably, no significant separation was observed between FruR and FruB at the PCA2 level, unlike that between MycR and MycB (Figure 2e,f). In addition, the heatmap cluster analysis showed that samples from the same *P. ostreatus* group clustered together, with differences observed between the light groups and the darkness group (Figure S2). In conclusion, different light qualities significantly affected the protein expression profiles. Specifically, the most significant differences in the mycelial samples were detected between white and blue light, whereas the fruiting body groups displayed notable disparities between white and red light.

Identification of the DEPs. Proteins with fold change in abundance >2 and a p-value <0.05 were screened as DEPs, which were distinguished from regular proteins through volcano plots (Figure S3). The comparison of the MycB vs MycD group showed the most DEPs in the mycelial samples (318), followed by the comparison of the MycR vs MycD group (280) (Figure 3a). In the fruiting body samples, the comparison of FruW vs the FruD group showed the most DEPs (313) while the comparison of the FruB vs FruR group displayed the fewest (95), particularly downregulated DEPs (Figure 3a). Subsequently, 692 and 619 nonredundant DEPs were obtained after merging the shared DEPs between each comparison by a Venn diagram for the samples from the mycelial and fruiting body stages, respectively (Figure 3b,c and Tables S2 and S3). Their expression is documented by a heatmap (Figure S4a,b). Further analysis of the 692 DEPs from the mycelial samples and the 619 DEPs from the fruiting body samples revealed a total of 1100 DEPs after merging, among which 211were shared (Figure 3d and Table S4). The abundance of the 211 DEPs, as illustrated by a heat map, revealed a division between DEPs from the mycelial and fruiting body stages (Figure S4). Additionally, significant differences were detected between the light groups and the darkness group within each stage (Figure S4c), indicating that light affects specific proteins at different developmental stages and certain proteins were responsive to light at both stages but likely with different expression levels.

GO Analysis for the DEPs. We conducted GO enrichment analysis within the comparisons between the light and dark groups to determine the physiological functions of the DEPs. First, all 1100 DEPs were involved in 14 "cellular component" (CC), 11 "molecular function" (MF), and 17 "biological process" (BP). Level 2 of the GO term enrichment was further analyzed for in-depth functional illustration within each comparison (Tables S5−S10), and the results are shown in Figure 4a and Figure S5. Based on the number of DEPs classified into each category, the largest upregulated and downregulated GO terms enriched in the three categories followed the

https://doi.org/10.1021/acs.jafc.3c06083
J. Agric. Food Chem. 2024, 72, 1361−1375

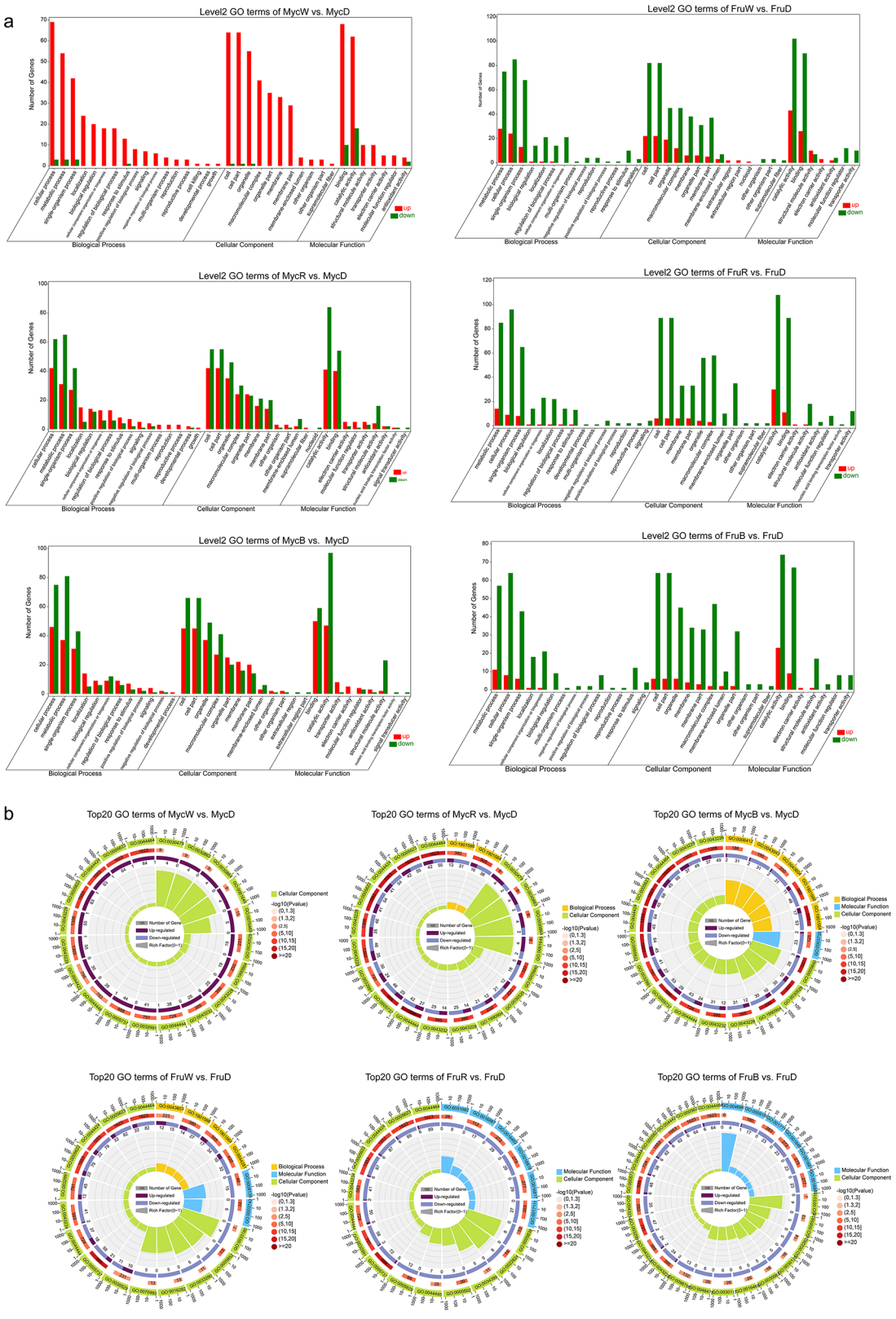

Figure 4. GO enrichment analysis of the DEPs from each comparison, MycW vs MycD, MycR vs MycD, FruW vs FruD, FruR vs FruD, and FruB vs FruD, respectively. (a) Level 2 of the GO term enrichment for each comparison. The red columns indicate the upregulated DEPs, and the green ones indicate the downregulated DEPs. (b) Circle map description of the top 20 of the GO enrichment terms for each comparison, respectively.

comparisons of the mycelial and fruiting body stages, including cellular process, metabolic process, single-organism process, localization, and cellular component organization and biogenesis for BP; the cell, cell part, organelle, macromolecular complex, organelle part, membrane, and membrane part for CC; and binding, catalytic activity, structural molecule activity, and transporter activity for MF. The majority of the GO terms for the MycW and MycD comparison were upregulated. However,

https://doi.org/10.1021/acs.jafc.3c06083
J. Agric. Food Chem. 2024, 72, 1361−1375

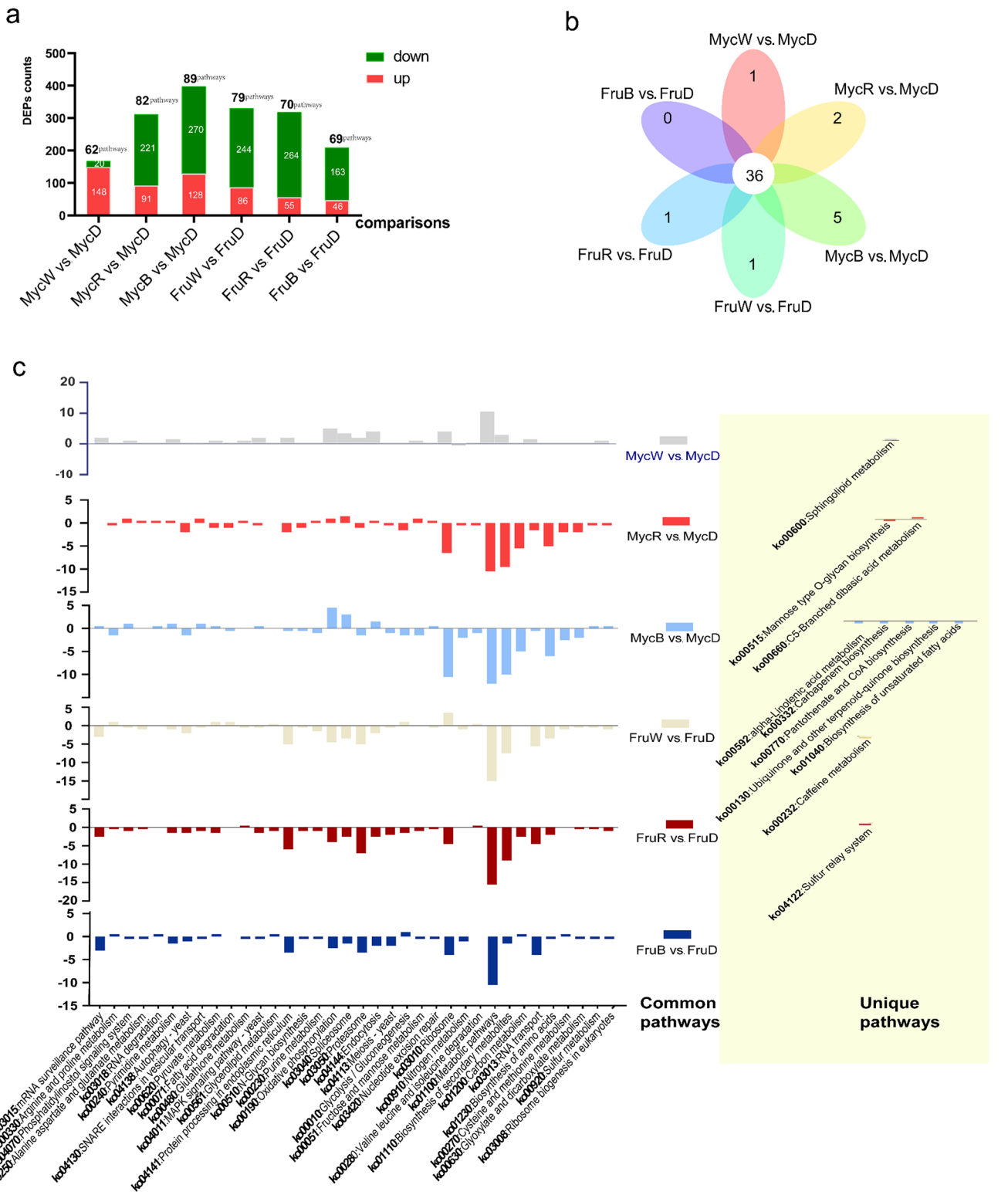

Figure 5. Statistic and distribution of enriched KEGG pathways of different comparisons. (a) Statistic of the upregulated and downregulated DEPs that were enriched in the relative KEGG pathways of each comparison. The number of pathways involved was listed on the top. (b) Venn diagram for the number of unique and common pathways of all the comparisons. (c) Statistic of the number of upregulated and downregulated DEPs for the 36 common pathways (left) and unique pathways (right) of each comparison.

the majority of the GO terms were downregulated when comparing the FruW to FruD, FruR to FruD, and FruB to FruD. In contrast, the MycR vs MycD and MycB vs MycD GO terms were relatively equally upregulated and downregulated between the comparisons (Figure 4a).

The top 20 GO enrichment terms are illustrated in a circle map (Figure 4b and Figure S5b). All comparisons were enriched mostly in CC terms with great variations in the MF and BP terms. In particular, the MycW vs MycD comparison was completely enriched with CC terms. The seven most common

https://doi.org/10.1021/acs.jafc.3c06083
J. Agric. Food Chem. 2024, 72, 1361−1375

GO terms belong to the CC category in all comparisons. Another six common CC terms were found in the MycW vs MycD, MycR vs MycD, and MycB vs MycD comparisons. However, only one CC term was found in the FruW vs FruD, FruR vs FruD, and FruB vs FruD comparisons (Figure 4b and Figure S5b). This suggests that the influence of different light qualities was more obvious during the fruiting body stage. Furthermore, BP terms were found in the MycR vs MycD, MycB vs MycD, and FruW vs FruD comparisons. The MF terms were remarkably enriched in the FruR vs FruD and FruB vs FruD comparisons, with four common terms, suggesting that red and blue light have more in common that affect the GO terms. Taken together, the different light qualities induced upregulated and downregulated DEPs in the *P. ostreatus* proteome with common and different terms in all three GO categories. All light treatments revealed differences in CC function in the top 20 enriched terms. Thus, we speculated that the different qualities of light exert mainly through the biological functions of CC to distinguish it from the darkness. The red and blue lights, compared to the white light, tended to affect a wider range of biological functions, including the CC, MF, and BP terms (Figure 4b). Notably, most of the biological functions were downregulated by light treatments during the fruiting body stage (Figure 4a). Moreover, the protein expression differences induced by light exposure during the mycelial and fruiting body stages were most pronounced under white light (Figure 4a).

KEGG Pathway Enrichment Analysis of the DEPs. The KEGG pathways of the DEPs were analyzed, and all DEPs were ascribed into five KEGG A classes and 19 B classes (Figure S6). The common pathways within each comparison contributed to the understanding of the effects of light on *P. ostreatus*. The MycW vs MycD comparison displayed the fewest DEPs in the "carbohydrate metabolism", "amino acid metabolism", and "translation" categories among all comparisons, probably corresponding to rapid growth of the mycelia under the white light and darkness conditions. The "Biosynthesis of other secondary metabolism" term was found in the MycR vs MycD, MycB vs MycD, and FruW vs FruD comparisons, indicating that light has an opposite effect on the biosynthesis of other secondary metabolites between the mycelial and fruiting body stages.

The statistics of the pathways and associated number of DEP are shown in Figure 5a. The DEPs were mostly downregulated among the various pathways in the light-treated groups, except MycW vs MycD, which showed the fewest pathways (62) (associated with 148 up- and 20 downregulated DEPs). This result verifies that the difference between white light and darkness was the least compared to the effect of red/blue light on *P. ostreatus* mycelial growth. The MycB vs MycD comparison displayed the greatest number of pathways (89), while the FruB vs FruD comparison showed far fewer pathways (69), indicating that blue light has a more significant effect on the mycelial pathways than those of fruiting bodies. Furthermore, 36 shared pathways were found among all comparisons and unique pathways were identified via a Venn diagram (Figure 5b and Table S11). White light mainly upregulated the 36 shared pathways during the mycelial stage, while red and blue light mainly downregulated them (Figure 5c). However, all three light conditions downregulated these pathways during the fruiting body stage (Figure 5c). In particular, the ribosome (ko03010) pathway was upregulated by white light and downregulated by red and blue light during both the mycelial and fruiting body stages. The purine metabolism (ko00230), oxidative phosphorylation (OXPHOS) (ko00190), and endocytosis (ko04144) pathways were upregulated at the mycelial stage and downregulated at the fruiting body stage under all light conditions. In addition, the unique pathways of the three comparisons showed only one upregulated or downregulated DEP (Figure 5c).

Furthermore, we focused on the top 20 pathways for each comparison, and the pathways that were shared are marked in red in Figure S7. OXPHOS (ko00190) and ribosome (ko03010) were commonly and significantly enriched in all comparisons. The carbon metabolism (ko01200) pathway was significantly enriched under all light conditions at the mycelial stage, while the pathways of the mRNA surveillance pathway (ko03015), proteasome (ko03050), and RNA transport (ko03013) were significantly enriched under all light conditions at the fruiting body stage (Figure S7). Other differentially expressed pathways, such as thiamine metabolism (ko00730), phagosome (ko04145), terpenoid backbone biosynthesis (ko00900), mannose type *O*-glycan biosynthesis (ko00515), and caffeine metabolism (ko00232) are illustrated in Figure S7.

qRT-PCR Validation of the Proteomic Data. The expression profiles obtained by proteomics were validated by qRT-PCR analysis. Genes related to the enriched pathways mentioned above, particularly those that showed significant changes under the different light treatments, as well as the light receptor proteins were selected. The qRT-PCR data were very consistent with the proteomic data in all comparisons (Figure S8), suggesting that the proteomic data were reliable.

DISCUSSION

Differences in the Proteomic Profiles under the Different Light Treatments. The effects of light have been extensively investigated in certain model fungal species, including *Aspergillus nidulans*, *Neurospora crassa*, *Coprinus cinereus*, and *L. edodes*.[11,45−48] However, mushroom species demonstrate diverse growth responses to distinct light qualities. Some species exhibit improved growth under blue light, while others thrive under red or white light conditions.[20,26,30,39] In this study, we investigated the protein profiles of *P. ostreatus* mycelial and fruiting bodies in response to different light qualities. The proteomics data revealed a diverse range of proteins under the light treatments, with the number varying between 46 and 155 for the mycelial samples and between 22 and 253 for the fruiting body samples. Notably, the dark group exhibited the highest abundance of unique proteins, followed by the white light group, indicating that exposure to different light qualities affects the expression of specific proteins (Figure 2). These findings follow previous studies on different basidiomycetes.[17,39]

Furthermore, when comparing the proteomic profiles between the light conditions and darkness, we identified many DEPs using a volcano plot with a cutoff of 2.0-fold change and a p-value <0.05. Light-signaling pathways are closely associated with biological pathways, including sporulation, primary metabolic pathways, and the production of secondary metabolites or hydrolytic enzymes.[5] The KEGG pathway analysis of these DEPs revealed a significant enrichment of the metabolic pathways. Interestingly, the differences in the pathways affected by the different light qualities were more pronounced during the *P. ostreatus* mycelial stage than during the fruiting body stage (Figure 5). Specifically, distinct differences were observed between the white and red light groups and most pathways were downregulated by blue and red

https://doi.org/10.1021/acs.jafc.3c06083
J. Agric. Food Chem. 2024, 72, 1361−1375

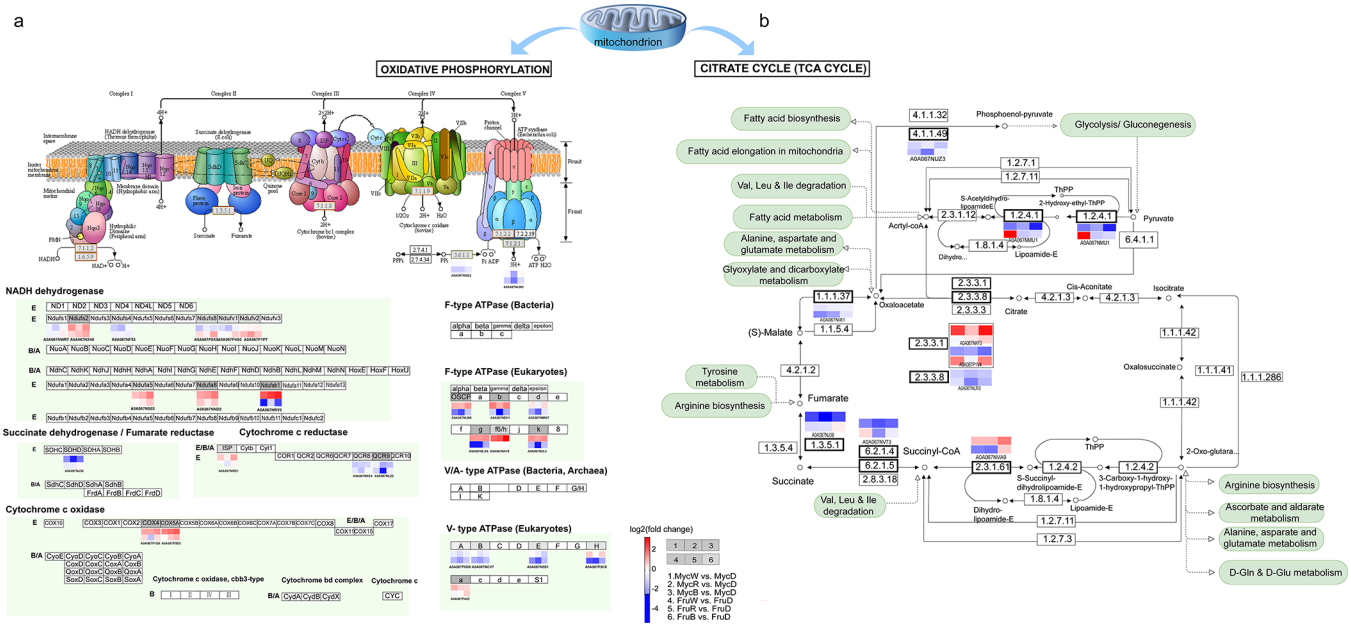

Figure 6. The expression analysis of DEPs related to the energy supply pathways. (a) DEPs located in the oxidative phosphorylation (ko00190) pathway of each light sample. The enzymes that were involved in the DEPs are marked with a gray box. (b) DEPs located in the TCA cycle (ko00020) of each light sample. The enzymes that were involved in the DEPs are marked with bold box lines. The corresponding change of protein expression of each DEP in all is displayed by heatmap using log2(fold change). The color indicators for log2(fold change) together with the organization of color-coded frames for sample comparations are shown in the middle bottom. MycW vs MycD, MycR vs MycD, and MycB vs MycD are short for the comparisons in the mycelium stage: W for the white light group, R for the red light group, B for the blue light group, and D for the darkness group; FruW vs FruD, FruR vs FruD, and FruB vs FruD are short for the comparisons from those in the fruiting body stage.

light (Figures 6 and Figures S5 and S6). Notably, light receptor proteins have specific functions during light exposure.[11,45−47,49] However, the protein expression analysis here did not detect the expression of light receptor proteins, including white collar 1 protein (A0A067P6 × 7) or the phytochrome B region (A0A067NQM3), in any of the groups. This result suggests that these specific *P. ostreatus* light receptor proteins have low expression levels, which were confirmed by qRT-PCR (Figure S8).

Significant Differences in the DEPs between the Mycelial Stage and the Fruiting Body Stage under White Light. White light exposure resulted in the highest expression of unique proteins compared to red and blue light (Figures 2 and 3) with significant differences in the DEPs during the mycelial and fruiting body stages (Figures 4 and 5). Specifically, the majority of the GO terms and KEGG pathways enriched in DEPs induced by white light were upregulated during the mycelial stage, while they were predominantly downregulated during the fruiting body stage. This result indicates distinct biological and metabolic patterns between the mycelial and fruiting body stages. The transition from a vegetative mycelium to a primordium is a complex and crucial developmental event in the life cycle of fruiting bodies in many basidiomycete fungi.[50,51] Light stimulates the production of biochemical substances involved in the formation of the *P. ostreatus* fruiting bodies.[52] Here, DEPs related to metabolic pathways (ko00010) and the biosynthesis of secondary metabolites (ko01110) showed opposite regulatory directions in the mycelium and fruiting bodies (Figure 5). Therefore, *P. ostreatus* may regulate different metabolic pathways in different developmental stages in response to white light. This may be attributed to the DEPs involved in the pathways, such as the OXPHOS pathway (ko00190), the tricarboxylic acid (TCA) cycle (ko00020), the proteasome pathway (ko03050), the mRNA surveillance pathway (ko03015), the pyruvate metabolism (ko00620), and endocytosis (ko04144) according to the KEGG analysis (Figure 5).

Light Affects the Energy Supply-Related Pathways. The OXPHOS pathway (ko00190) occurs in the mitochondrion, plays a crucial role in energy (ATP) production, and is the principal energy metabolism in white-rot fungi.[53,54] The OXPHOS pathway shows enormous evolutionary plasticity in fungi, and the variations have adapted to different ecological niches.[55] This pathway participates in the blue light response process in *P. eryngii*.[20] In this study, the expression of 28 DEPs in this pathway was analyzed, which were related to NADH-ubiquinone oxidoreductase (9 proteins), succinate dehydrogenase (1 protein), cytochrome c reductase (3 proteins), cytochrome c oxidase (2 proteins), ATP synthase (11 genes), inorganic diphosphatase (1 protein), and plasma membrane ATPase (1 protein) (Figure 6a). These proteins play key roles in the mitochondrial electron transport chain, which drives oxidative phosphorylation. Four proteins (A0A067P1P7, A0A067NX49, AOA067NS03, and AOA067NND2) related to NADH-quinone oxidoreductases (Ndufv2, Ndufs2, Ndufa5, and Ndufa8) were upregulated by all of the light treatments during both stages, indicating that electron transport may be strengthened when OXPHOS is induced by light. However, A0A067NRY0, which is related to the acyl carrier protein (ACP), exhibited contrasting up-regulation and downregulation during the mycelial and fruiting body stages, respectively, under the same light conditions. The downregulation of ACP during the fruiting body stage by white/blue light may contribute to the development of the fruiting body, as ACP in mitochondria plays a crucial role in fatty acid synthesis.[56] Succinate dehydrogenase is a mitochondrial marker enzyme positioned between

https://doi.org/10.1021/acs.jafc.3c06083
J. Agric. Food Chem. 2024, 72, 1361−1375

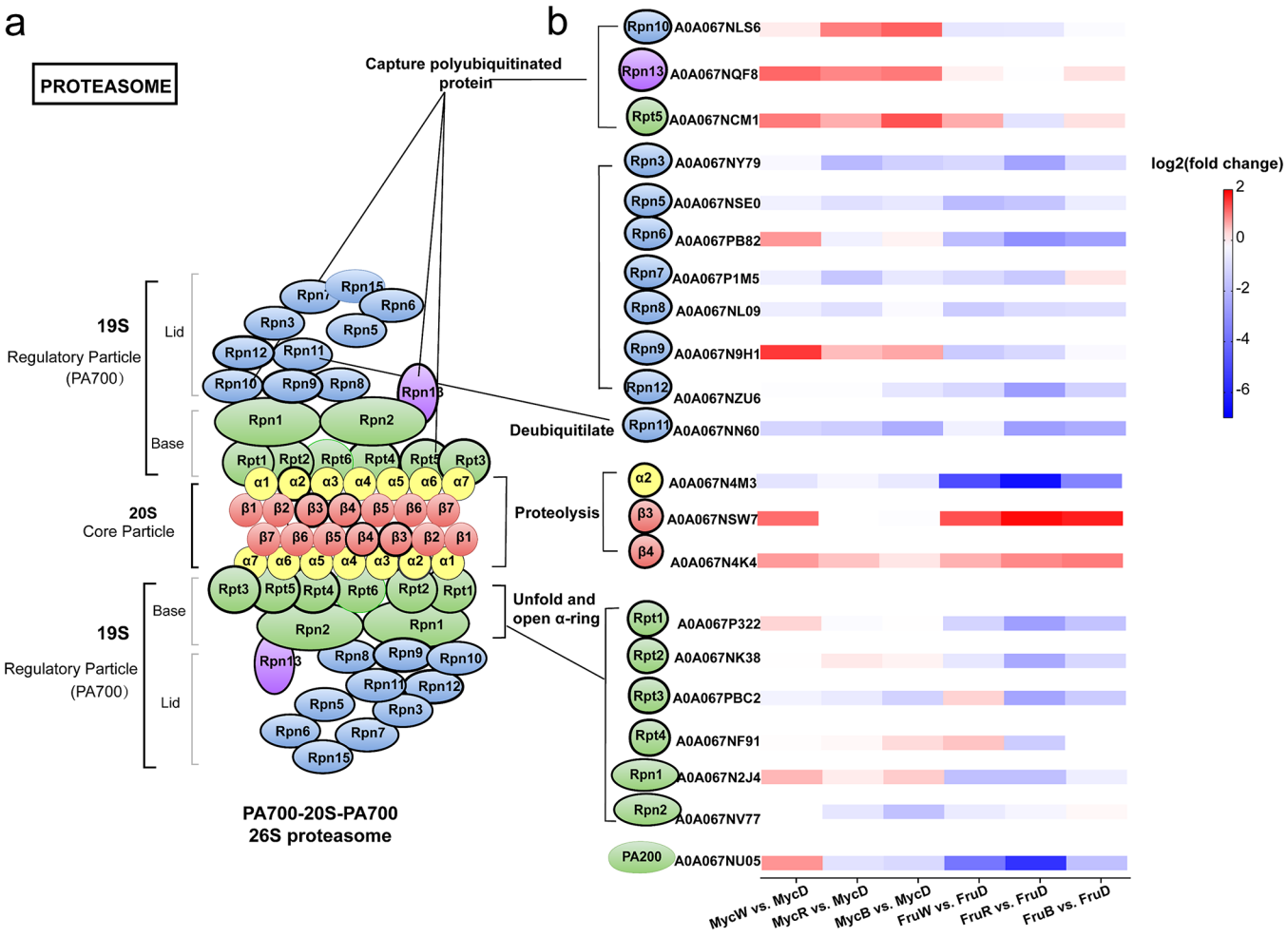

Figure 7. The expression analysis of DEPs located in ko03050 (proteasome pathway) of all comparisons. (a) Composition of the 26S proteasome and the expression analysis of the DEPs in proteasome pathway. (b) The 21 DEPs are marked with bold outline, and their expression changes in all comparisons are displayed with the color indicator for the log2(fold change) at the right.

phosphorylation of the OXPHOS and electron transport, and it is also linked to the TCA cycle. Cytochrome c reductase may provide essential energy for the TCA cycle. However, succinate dehydrogenase complex D of succinate dehydrogenase and QCR8/QCR9 of cytochrome c reductase were downregulated under all light treatments, particularly red light. Moreover, the DEPs induced by red light in the TCA cycle (Figure 6b) were all downregulated in the FruR vs FruD comparison, indicating inhibition of the TCA cycle by red light. Pyruvate dehydrogenase [EC: 1.2.4.1] in the TCA cycle was highly upregulated in the FruW vs FruD comparison (Figure 6b), which may have caused decarboxylation of pyruvate to produce acetyl-CoA, which facilitates various metabolic pathways. In addition, the expression changes in the DEPs of the OXPHOS pathway revealed that red light induced quite a different overall expression trend compared to the white and blue light treatments in both stages of *P. ostreatus* (Figure 6a). Another interesting result was that most ATP synthase DEPs were upregulated during the mycelial stage, which contributed to an adequate ATP supply. However, white and blue light were more effective than red light. We speculated that the cumulative light effects of these two stages lead to an inadequate ATP supply under red light, resulting in an inferior yield and size of *P. ostreatus*.

Light Affects the Ubiquitin−Proteasome System (UPS). The UPS is the major pathway regulating cellular proteolysis and plays a crucial role in the cell response to various environmental stressors, such as nutrient limitations, heat shock, and heavy metal exposure.[57,58] The response leads to the degradation of proteins and changes in the rate of intracellular protein turnover, among which the 26S proteasome is involved in the majority of regulated protein catabolism.[59] In this study, 21 DEPs enriched in the proteasome pathway (ko03050) were identified in *P. ostreatus* under light treatments by KEGG analysis. Among them, 18 DEPs were reflected in 19S regulatory particle with 9 in Lid and 9 in Base, whereas only 3 DEPs were reflected in the 20S core particle as $\alpha 2$, $\beta 3$, and $\beta 4$ (Figure 7). The proteasome subunit beta [EC: 3.4.25.1], composed of $\beta 3$ and $\beta 4$, was upregulated in response to all light treatments, and white light had a particularly pronounced effect compared to darkness. The proteins related to Rpn10, Rpn13, and Rpt5, which are responsible for capturing polyubiquitinated proteins, were all upregulated by white and blue light during both stages but downregulated by red light during the fruiting body stage. These findings indicate that white light significantly enhances the UPS process. The 19S regulatory particle was comprehensively affected by the different light treatments. Eight lid-related proteins, namely, Rpn3, Rpn5, Rpn6, Rpn7, Rpn8, Rpn9, Rpn 11, and Rpn12, were mostly downregulated, except Rpn6 and

https://doi.org/10.1021/acs.jafc.3c06083
J. Agric. Food Chem. 2024, 72, 1361−1375

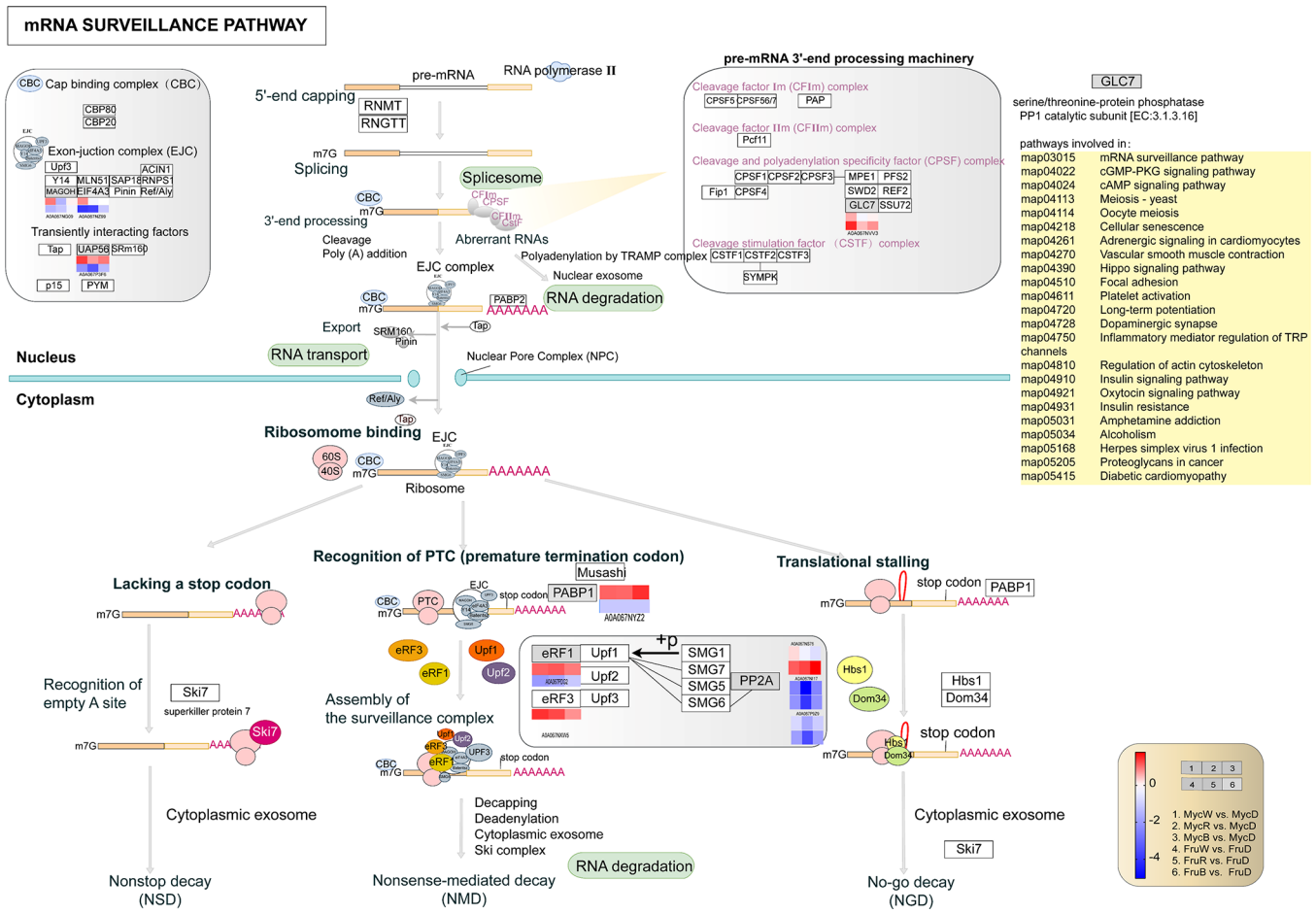

Figure 8. The expression analysis of DEPs located in ko03015 (mRNA surveillance pathway) of each light sample. The enzymes that were involved in the DEPs are marked in gray box. The corresponding change of protein expression of each DEP in all comparisons is displayed by heatmap using log2(fold change). The color indicator for log2(fold change) and the organization of color-coded frames for sample comparations are shown on the lower right corner.

Rnp9 in the MycW group that were upregulated. Six base-related DEPs, namely, Rpt1, Rpt2, Rpt3, Rpt4, Rpn1, and Rpn2, were upregulated during the mycelial stage but downregulated during the fruiting body stage. In particular, the MycW group was upregulated while the FruR group was significantly downregulated. The downregulation of PA200 in the FruR group may have decreased the rate of proteasomal degradation and inhibited cell growth, as PA200 in yeast plays a role in DNA repair.[60] The comparison of DEPs in the 19S particle subunits further indicated the promotive effect of white light and the inhibitory effect of red light during the *P. ostreatus* fruiting body stage. The effect of the light signal on the stability of proteins in the proteasome pathway has been well studied in fungi, such as *Trichoderma reesei*, as well as in white-rot basidiomycetes, such as *C. unicolor* and *H. marmoreus*, revealing that various genes are involved in proteolysis in response to light and proteases, which serve as regulatory molecules.[39,57,61] However, the significance of regulating protease activities with light remains largely unclear and further studies are needed.

Light Affects the mRNA Surveillance Pathways. Eukaryotic cells contain translation-related mRNA surveillance pathways (ko03015) that effectively prevent the synthesis of potentially defective proteins resulting from abnormal mRNA translation events.[62,63] The DEPs related to the mRNA surveillance pathway are illustrated in Figure 8. The A0A067NVV3 protein related to GLC7, which is involved in pre-mRNA 3′-end processing machinery, was upregulated in all comparisons with the highest fold change in the FruW vs FruD comparison (Figure 8). GLC7 is a catalytic subunit of the PP1 serine/threonine-protein phosphatase [EC: 3.1.3.16], which removes phosphate groups from proteins, thereby participating in cellular signal regulation, metabolic regulation, the cell cycle, and cell apoptosis, among other biological processes.[64] In addition, GLC7 has been extensively studied in *Saccharomyces cerevisiae*, where it is essential for maintaining cell wall integrity, regulating morphogenesis, and promoting cell cycle progression.[65−67] However, limited research is available on GLC7 in edible mushrooms. GLC7 is involved in 23 KEGG pathways, most of which are related to signaling pathways (Figure 8). Therefore, we speculate that the high expression of GLC7 induced by white light promoted intracellular signaling in *P. ostreatus*. Two proteins (eIF4A3 and MAGOH) related to the exon-junction complex (EJC) and one protein (UAP56) related to transiently interacting factors were significantly downregulated in the FruW vs FruD and FruR vs FruD comparisons than that of the FruB vs FruD comparison. In particular, the downregulation of eIF4A3 and UAP56 was evident in the FruR vs FruD comparison, indicating that red light may inhibit mRNA stability during the fruiting body stage. This would result in the generation of premature translation termination codons harboring mRNA, which would be rapidly degraded by the nonsense-mediated mRNA decay (NMD) pathway.[68] The

https://doi.org/10.1021/acs.jafc.3c06083
J. Agric. Food Chem. 2024, 72, 1361−1375

NMD pathway has three factors as core components, namely, Upf1p, Upf2p/Nmd2p, and Upf3p.[69] However, activating the NMD pathway requires recognition of a premature stop codon by a termination complex comprising eRF1 and eRF3. eRF1 recognizes the three stop codons and triggers the release of the newly synthesized polypeptide chain. eRF3 is a GTPase hydrolyzes of GTP to facilitate the stop codon decoded by eRF1.[68] Interactions between eRF3 and Upf1p have been described in yeast and human cells.[70−72] Less is known about the interactions between eRF1 and Upf1p. Here, eRF1 was downregulated and eRF3 was not expressed in the fruiting body samples, revealing a deficiency in assembly of the surveillance complex. Moreover, the EJC/CBC branch of the NMD pathway, including the eIF4A3 as the EJC core component and eRF1 recognizing the termination codons, regulates mRNA stability in the filamentous fungus *N. crassa*.[73] These results suggest the important roles of eIF4A3 and eRF1 in the *P. ostreatus* light response.

Light Induces Other Metabolic Proteins. Two enzymes, namely, glutamine synthetase (GS; [EC: 6.3.1.2]) and aldehyde dehydrogenase (ALDH; [EC: 1.2.1.3]), changed significantly under different light treatments (Figure S8). GS is a critical enzyme that catalyzes the conversion of glutamate to glutamine, which serves as a metabolic precursor of numerous essential nitrogen metabolites in yeast and filamentous fungi.[74−76] The *P. ostreatus* protein AOA067NQW2 related to GS and was downregulated the most with an 8.4-fold change in the FruR vs FruD comparison, and it was downregulated by 2.6-fold and 3.2-fold in the FruW vs FruD and FruB vs FruD comparisons, respectively. This result suggests that red light significantly downregulates GS expression and affects a series of interconnected metabolic pathways. However, the biological function of GS extends beyond glutamine synthesis, as GS participates in ammonium sensing and transducing signals to nitrogen catabolite repressing genes in *Fusarium fujikuroi*[77] and regulates mycelial growth and biosynthesis of ganoderic acid in *Ganoderma lucidum*.[75] The AOA067NL74 protein, which is related to ALDH, was far more downregulated (by 3.4-fold) in the FruR vs FruD comparison, while the FruW vs FruD and FruB vs FruD comparisons were slightly downregulated by 0.7-fold and 0.9-fold, respectively. Notably, significant increases of 7.3-fold and 6.5-fold were observed in the MycW vs MycD and MycB vs MycD comparisons, but no increase was observed in the MycR vs MycD comparison. This finding indicates that red light inhibits the activity of ALDH, which engages in many cellular functions and is critical for cell survival and adaptation to cellular and environmental stress.[78,79]

In conclusion, the proteomic profiles of the *P. ostreatus* mycelia and fruiting bodies were comprehensively analyzed under different light treatments in this study. The metabolic pathways and crucial enzymes, such as OXPHOS, proteasome, and mRNA surveillance pathways, as well as GS and ALDH, discovered by the enrichment analysis provided insight into the mechanism of the light-induced effects on *P. ostreatus* growth during mycelial and fruiting body stages. Although no photoreceptors were detected with obvious differences in the proteomic analysis, the expression of white collar 1 protein was significantly enhanced under white light confirmed by qRT-PCR. These findings serve as a valuable resource for further research on this mushroom species and facilitate advancements in mushroom cultivation techniques.

■ ASSOCIATED CONTENT

Supporting Information

The Supporting Information is available free of charge at https://pubs.acs.org/doi/10.1021/acs.jafc.3c06083.

The fruiting body characters of *P. ostreatus* PH11 under different light qualities (Figure S1); heat map of the proteins in all samples of *P. ostreatus* (Figure S2); volcano plot of each comparison (Figure S3); heatmap generated from nonredundant DEPs (Figure S4); GO enrichment of each comparisons (Figure S5); distribution of KEGG pathways for different comparisons (Figure S6); top 20 enriched KEGG pathways of the DEPs for each comparison group (Figure S7); and qRT-PCR verification (Figure S8) (PDF)

Primers used in this study (Table S1); DEPs identified in mycelium and fruiting body samples of *P. ostreatus* (Tables S2 and S3); 1100 DEPs identified under different light conditions both in mycelium and fruiting body stages (Table S4); level 2 of GO annotation of DEPs for comparison of each light with darkness (Tables S5−S10); and unique and common pathways in each comparison (Table S11) (XLSX)

■ AUTHOR INFORMATION

Corresponding Authors

Song Yang − *Shandong Provincial Key Laboratory of Applied Mycology, School of Life Sciences, Qingdao Agricultural University, Qingdao, Shandong Province 266109, People's Republic of China*; orcid.org/0000-0002-4022-3941; Email: yangsong1209@163.com

Hao Yu − *Shandong Provincial Key Laboratory of Applied Mycology, School of Life Sciences, Qingdao Agricultural University, Qingdao, Shandong Province 266109, People's Republic of China*; Phone: +86-532-880-30373; Email: yuhaosunshine@163.com

Authors

Liping Zhu − *Shandong Provincial Key Laboratory of Applied Mycology, School of Life Sciences, Qingdao Agricultural University, Qingdao, Shandong Province 266109, People's Republic of China*; orcid.org/0000-0002-2255-5707

Yao Su − *Shandong Provincial Key Laboratory of Applied Mycology, School of Life Sciences, Qingdao Agricultural University, Qingdao, Shandong Province 266109, People's Republic of China*

Shunan Ma − *Shandong Provincial Key Laboratory of Applied Mycology, School of Life Sciences, Qingdao Agricultural University, Qingdao, Shandong Province 266109, People's Republic of China*

Lizhong Guo − *Shandong Provincial Key Laboratory of Applied Mycology, School of Life Sciences, Qingdao Agricultural University, Qingdao, Shandong Province 266109, People's Republic of China*

Complete contact information is available at: https://pubs.acs.org/10.1021/acs.jafc.3c06083

Author Contributions

#H.Y. and S.Y. conceived the project and designed the experiment. L.Z. and Y.S. performed the experiments. S.M. and L.G. assisted in statistical analyses. L.Z. wrote the original draft. H.Y. and S.Y. revised the paper. The final manuscript was read and approved by all authors.

Funding

This work was financially supported by the Key R&D Program of Shandong Province (2021ZDSYS28), National Natural Science Foundation of China (grant No. 31600028), High-level Talent Research Fund of Qingdao Agricultural University (663/1118011), and Qingdao Agricultural University Scientific Research Foundation (6602423332).

Notes

The authors declare no competing financial interest.

■ ABRREVIATIONS USED

M, mycelium growth stage; F, fruiting body stage; DEPs, differentially expressed proteins; MycW, sample of mycelium under white light; MycR, sample of mycelium under red light; MycB, sample of mycelium under blue light; FruW, sample of fruiting bodies under white light; FruR, sample of fruiting bodies under red light; FruB, sample of fruiting bodies under blue light; ACN, acetonitrile; rpm, revolutions per minute; MnP, manganese peroxidase; PBS, phosphate-buffered saline; MF, molecular function; CC, cellular component; BP, biological process; OXPHOS, oxidative phosphorylation; UPS, ubiquitin−proteasome system; ACP, acyl carrier protein; TCA cycle, tricarboxylic acid cycle; EJC, exon-junction complex; NMD, nonsense-mediated mRNA decay; GS, glutamine synthetase; ALDH, aldehyde dehydrogenase; qRT-PCR, quantitative real-time polymerase chain reaction

■ REFERENCES

(1) Sakamoto, Y. Influences of environmental factors on fruiting body induction, development and maturation in mushroom-forming fungi. *Fungal Biol. Rev.* **2018**, *32* (4), 236−248.

(2) Kĕes, U.; Liu, Y. Fruiting body production in basidiomycetes. *Appl. Microbiol. Biotechnol.* **2000**, *54* (2), 141−152.

(3) Bracker, L. B.; Siju, K. P.; Varela, N.; Aso, Y.; Zhang, M.; Hein, I.; Vasconcelos, M. L.; Grunwald Kadow, I. C. Essential role of the mushroom body in context-dependent CO(2) avoidance in Drosophila. *Curr. Biol.* **2013**, *23* (13), 1228−34.

(4) Tisch, D.; Schmoll, M. Light regulation of metabolic pathways in fungi. *Appl. Microbiol. Biotechnol.* **2010**, *85* (5), 1259−77.

(5) Yu, Z.; Fischer, R. Light sensing and responses in fungi. *Nat. Rev. Microbiol* **2019**, *17* (1), 25−36.

(6) Sakamoto, Y.; Sato, S.; Ito, M.; Ando, Y.; Nakahori, K.; Muraguchi, H. Blue light exposure and nutrient conditions influence the expression of genes involved in simultaneous hyphal knot formation in Coprinopsis cinerea. *Microbiol Res.* **2018**, *217*, 81−90.

(7) Janusz, G.; Sulej, J.; Jaszek, M.; Osińska-Jaroszuk, M. Effect of different wavelengths of light on laccase, cellobiose dehydrogenase, and proteases produced by Cerrena unicolor, Pycnoporus sanguineus and Phlebia lindtneri. *Acta Biochim. Pol.* **2016**, *63* (2), 223−228.

(8) Mei, X. L.; Zhao, Z.; Chen, X. D.; Lan, J. Light quality regulation of growth and endogenous IAA metabolism of Ganoderma lucidum mycelium. *Zhongguo Zhongyao Zazhi* **2013**, *38* (12), 1887−92.

(9) Kamada, T.; Sano, H.; Nakazawa, T.; Nakahori, K. Regulation of fruiting body photomorphogenesis in Coprinopsis cinerea. *Fungal Genet Biol.* **2010**, *47* (11), 917−21.

(10) Gornostai, T. G.; Borovskii, G. G.; Kashchenko, N. I.; Olennikov, D. N. Phenolic Compounds of Inonotus rheades (Agaricomycetes) Mycelium: RP-UPLC-DAD-ESI/MS Profile and Effect of Light Wavelength on Styrylpyrone Content. *Int. J. Med. Mushrooms* **2018**, *20* (7), 637−645.

(11) Kim, J. Y.; Kim, D. Y.; Park, Y. J.; Jang, M. J. transcriptome analysis of the edible mushroom Lentinula edodes in response to blue light. *PLoS One* **2020**, *15* (3), No. e0230680.

(12) Tang, L. H.; Tan, Q.; Bao, D. P.; Zhang, X. H.; Jian, H. H.; Li, Y.; Yang, R. H.; Wang, Y. Comparative Proteomic Analysis of Light-Induced Mycelial Brown Film Formation in Lentinula edodes. *Biomed Res. Int.* **2016**, *2016*, 5837293 DOI: 10.1155/2016/5837293.

(13) Huang, X.; Zhang, R.; Qiu, Y.; Wu, H.; Xiang, Q.; Yu, X.; Zhao, K.; Zhang, X.; Chen, Q.; Penttinen, P.; Gu, Y. RNA-seq Profiling Showed Divergent Carbohydrate-Active Enzymes (CAZymes) Expression Patterns in Lentinula edodes at Brown Film Formation Stage Under Blue Light Induction. *Front. Microbiol.* **2020**, *11*, 1044.

(14) Tang, L. H.; Jian, H. H.; Song, C. Y.; Bao, D. P.; Shang, X. D.; Wu, D. Q.; Tan, Q.; Zhang, X. H. transcriptome analysis of candidate genes and signaling pathways associated with light-induced brown film formation in Lentinula edodes. *Appl. Microbiol. Biotechnol.* **2013**, *97* (11), 4977−89.

(15) Park, Y. J.; Jang, M. J. Blue Light Induced Edible Mushroom (Lentinula edodes) Proteomic Analysis. *J. Fungi* **2020**, *6* (3), 127 DOI: 10.3390/jof6030127.

(16) Wang, H.; Tong, X.; Tian, F.; Jia, C.; Li, C.; Li, Y. Transcriptomic profiling sheds light on the blue-light and red-light response of oyster mushroom (Pleurotus ostreatus). *AMB Express* **2020**, *10* (1), 10.

(17) Araujo, N. L.; Avelino, K. V.; Halabura, M. I. W.; Marim, R. A.; Kassem, A. S. S.; Linde, G. A.; Colauto, N. B.; do Valle, J. S. Use of green light to improve the production of lignocellulose-decay enzymes by Pleurotus spp. in liquid cultivation. *Enzyme Microb Technol.* **2021**, *149*, No. 109860.

(18) Ye, D.; Du, F.; Hu, Q.; Zou, Y.; Bai, X. transcriptome Analysis Reveals Candidate Genes Involved in Light-Induced primordium Differentiation in Pleurotus eryngii. *Int. J. Mol. Sci.* **2021**, *23* (1), 435 DOI: 10.3390/ijms23010435.

(19) Du, F.; Zou, Y.; Hu, Q.; Zhang, H.; Ye, D. Comparative transcriptomic analysis reveals molecular processes involved in pileus morphogenesis in Pleurotus eryngii under different light conditions. *Genomics* **2020**, *112* (2), 1707−1715.

(20) Xie, C.; Gong, W.; Zhu, Z.; Yan, L.; Hu, Z.; Peng, Y. Comparative transcriptomics of Pleurotus eryngii reveals blue-light regulation of carbohydrate-active enzymes (CAZymes) expression at primordium differentiated into fruiting body stage. *Genomics* **2018**, *110* (3), 201−209.

(21) Pawlik, A.; Mazur, A.; Wielbo, J.; Koper, P.; Zebracki, K.; Kubik-Komar, A.; Janusz, G. RNA Sequencing Reveals Differential Gene Expression of Cerrena unicolor in Response to Variable Lighting Conditions. *Int. J. Mol. Sci.* **2019**, *20* (2), 290 DOI: 10.3390/ijms20020290.

(22) Pawlik, A.; Ruminowicz-Stefaniuk, M.; Frac, M.; Mazur, A.; Wielbo, J.; Janusz, G. The wood decay fungus Cerrena unicolor adjusts its metabolism to grow on various types of wood and light conditions. *PLoS One* **2019**, *14* (2), No. e0211744.

(23) Pawlik, A.; Jaszek, M.; Swatek, A.; Ruminowicz-Stefaniuk, M.; Ciolek, B.; Mazur, A.; Janusz, G. Lighting Conditions Influence the Dynamics of Protease Synthesis and Proteasomal Activity in the White Rot Fungus Cerrena unicolor. *Biomolecules* **2020**, *10* (9), 1322 DOI: 10.3390/biom10091322.

(24) Jang, M. J.; Lee, Y. H.; Ju, Y. C.; Kim, S. M.; Koo, H. M. Effect of Color of Light Emitting Diode on Development of Fruit Body in Hypsizygus marmoreus. *Mycobiology* **2013**, *41* (1), 63−6.

(25) Huang, M.-Y.; Lin, K.-H.; Lu, C.-C.; Chen, L.-R.; Hsiung, T.-C.; Chang, W.-T. The intensity of blue light-emitting diodes influences the antioxidant properties and sugar content of oyster mushrooms (Lentinus sajor-caju). *Scientia Horticulturae* **2017**, *218*, 8−13.

(26) Yue, Z.; Zhang, W.; Liu, W.; Xu, J.; Liu, W.; Zhang, X. Effect of Different Light Qualities and Intensities on the Yield and Quality of Facility-Grown Pleurotus eryngii. *J. Fungi* **2022**, *8* (12), 1244 DOI: 10.3390/jof8121244.

(27) Yang, T.; Dong, C. Photo morphogenesis and photo response of the blue-light receptor gene Cmwc-1 in different strains of Cordyceps militaris. *FEMS Microbiol Lett.* **2014**, *352* (2), 190−7.

(28) Sanchez, C. Cultivation of Pleurotus ostreatus and other edible mushrooms. *Appl. Microbiol. Biotechnol.* **2010**, *85* (5), 1321−37.

(29) Zawadzka, A.; Janczewska, A.; Kobus-Cisowska, J.; Dziedzinski, M.; Siwulski, M.; Czarniecka-Skubina, E.; Stuper-Szablewska, K. The effect of light conditions on the content of selected active ingredients in

anatomical parts of the oyster mushroom (Pleurotus ostreatus L.). *PLoS One* **2022**, *17* (1), No. e0262279, DOI: 10.1371/journal.pone.0262279.
(30) Nakano, Y.; Fujii, H.; Kojima, M. Identification of blue-light photoresponse genes in oyster mushroom mycelia. *Biosci Biotechnol Biochem* **2010**, *74* (10), 2160−5.
(31) Kojima, M.; Kimura, N.; Miura, R. Regulation of primary metabolic pathways in oyster mushroom mycelia induced by blue light stimulation: accumulation of shikimic acid. *Sci. Rep.* **2015**, *5*, 8630.
(32) Zhu, W.; Hu, J.; Li, Y.; Yang, B.; Guan, Y.; Xu, C.; Chen, F.; Chi, J.; Bao, Y. Comparative Proteomic Analysis of Pleurotus ostreatus Reveals Great Metabolic Differences in the Cap and Stipe Development and the Potential Role of Ca(2+) in the primordium Differentiation. *Int. J. Mol. Sci.* **2019**, *20* (24), 6317 DOI: 10.3390/ijms20246317.
(33) Zou, Y.; Zhang, M.; Qu, J.; Zhang, J. iTRAQ-Based Quantitative Proteomic Analysis Reveals Proteomic Changes in Mycelium of Pleurotus ostreatus in Response to Heat Stress and Subsequent Recovery. *Front. Microbiol.* **2018**, *9*, 2368.
(34) Lin, R.; Zhang, L.; Yang, X.; Li, Q.; Zhang, C.; Guo, L.; Yu, H.; Yu, H. Responses of the Mushroom Pleurotus ostreatus under Different CO(2) Concentration by Comparative Proteomic Analyses. *J. Fungi (Basel)* **2022**, *8* (7), 652 DOI: 10.3390/jof8070652.
(35) Elhusseiny, S. M.; El-Mahdy, T. S.; Awad, M. F.; Elleboudy, N. S.; Farag, M. M. S.; Yassein, M. A.; Aboshanab, K. M. Proteome Analysis and In Vitro Antiviral, Anticancer and Antioxidant Capacities of the Aqueous Extracts of Lentinula edodes and Pleurotus ostreatus Edible Mushrooms. *Molecules* **2021**, *26* (15), 4623 DOI: 10.3390/molecules26154623.
(36) Yang, X.; Lin, R.; Xu, K.; Guo, L.; Yu, H. Comparative Proteomic Analysis within the Developmental Stages of the Mushroom White Hypsizygus marmoreus. *J. Fungi* **2021**, *7* (12), 1064 DOI: 10.3390/jof7121064.
(37) Xu, L.; Gao, J.; Guo, L.; Yu, H. Heat shock protein 70 (HmHsp70) from Hypsizygus marmoreus confers thermotolerance to tobacco. *AMB Express* **2020**, *10* (1), 12.
(38) Rappsilber, J.; Mann, M.; Ishihama, Y. Protocol for micro-purification, enrichment, pre-fractionation and storage of peptides for proteomics using StageTips. *Nat. Protoc* **2007**, *2* (8), 1896−906.
(39) Zhu, L.; Su, Y.; Ma, Z.; Guo, L.; Yang, S.; Yu, H. Comparative proteomic analysis reveals differential protein expression of Hypsizygus marmoreus in response to different light qualities. *Int, J. Biological Macromol.* **2022**, *223* (Pt A), 1320−1334.
(40) Van, P.; Jiang, W.; Gottardo, R.; Finak, G. ggCyto: next generation open-source visualization software for cytometry. *Bioinformatics* **2018**, *34* (22), 3951−3953.
(41) Ashburner, M.; Ball, C. A.; Blake, J. A.; Botstein, D.; Butler, H.; Cherry, J. M.; Davis, A. P.; Dolinski, K.; Dwight, S. S.; Eppig, J. T.; Harris, M. A.; Hill, D. P.; Issel-Tarver, L.; Kasarskis, A.; Lewis, S.; Matese, J. C.; Richardson, J. E.; Ringwald, M.; Rubin, G. M.; Sherlock, G. Gene ontology: tool for the unification of biology. The Gene Ontology Consortium. *Nat. Genet.* **2000**, *25* (1), 25−9.
(42) Kanehisa, M.; Goto, S.; Sato, Y.; Furumichi, M.; Tanabe, M. KEGG for integration and interpretation of large-scale molecular data sets. *Nucleic Acids Res.* **2012**, *40* (Database issue), D109−14.
(43) Mallak, A. M.; Lakzian, A.; Khodaverdi, E.; Haghnia, G. H.; Mahmoudi, S. Effect of *Pleurotus ostreatus* and *Trametes versicolor* on triclosan biodegradation and activity of laccase and manganese peroxidase enzymes. *Microb Pathogenesis* **2020**, *149*, No. 104473, DOI: 10.1016/j.micpath.2020.104473.
(44) Sakamoto, Y.; Tamai, Y.; Yajima, T. Influence of light on the morphological changes that take place during the development of the Flammulina velutipes fruit body. *Mycoscience* **2004**, *45* (5), 333−339.
(45) Chen, C. H.; Loros, J. J. Neurospora sees the light: light signaling components in a model system. *Commun. Integr Biol.* **2009**, *2* (5), 448−51.
(46) Idnurm, A.; Heitman, J. Light controls growth and development via a conserved pathway in the fungal kingdom. *PLoS Biol.* **2005**, *3* (4), No. e95.
(47) Yu, Z.; Streng, C.; Seibeld, R. F.; Igbalajobi, O. A.; Leister, K.; Ingelfinger, J.; Fischer, R. Genome-wide analyses of light-regulated genes in Aspergillus nidulans reveal a complex interplay between different photoreceptors and novel photoreceptor functions. *PLoS Genet* **2021**, *17* (10), No. e1009845.
(48) Terashima, K.; Yuki, K.; Muraguchi, H.; Akiyama, M.; Kamada, T. The dst1 gene involved in mushroom photomorphogenesis of Coprinus cinereus encodes a putative photoreceptor for blue light. *Genetics* **2005**, *171* (1), 101−8.
(49) Sano, H.; Narikiyo, T.; Kaneko, S.; Yamazaki, T.; Shishido, K. Sequence analysis and expression of a blue-light photoreceptor gene, Le.phrA from the basidiomycetous mushroom Lentinula edodes. *Biosci Biotechnol Biochem* **2007**, *71* (9), 2206−13.
(50) Cheng, C. K.; Au, C. H.; Wilke, S. K.; Stajich, J. E.; Zolan, M. E.; Pukkila, P. J.; Kwan, H. S. 5′-Serial Analysis of Gene Expression studies reveal a transcriptomic switch during fruiting body development in Coprinopsis cinerea. *BMC Genom.* **2013**, *14*, 195.
(51) Duan, C.; Yao, L.; Lv, J. H.; Jia, C. W.; Tian, F. H.; Li, C. T. Systematic analysis of changes across different developmental stages of the mushroom Sarcomyxa edulis. *Gene* **2022**, *824*, No. 146450.
(52) Lee, S. R.; Joo, W. J.; Baek, Y. U.; Kim, I.; Chay, K. O.; Cho, S. H.; Lee, S. J.; Kang, S. O. Effect of light and reductones on differentiation of Pleurotus ostreatus. *J. Microbiol* **2011**, *49* (1), 71−7.
(53) Wilson, D. F. Oxidative phosphorylation: regulation and role in cellular and tissue metabolism. *J. Physiol* **2017**, *595* (23), 7023−7038.
(54) Li, W.; Wang, S.; Chen, Y.; Liu, L.; Hou, S.; You, H. Integration of transcriptomic and proteomic reveals the toxicological molecular mechanisms of decabromodiphenyl ethane (DBDPE) on Pleurotus ostreatus. *Environ. Pollut.* **2022**, *314*, No. 120263.
(55) Lavin, J. L.; Oguiza, J. A.; Ramirez, L.; Pisabarro, A. G. Comparative genomics of the oxidative phosphorylation system in fungi. *Fungal Genet Biol.* **2008**, *45* (9), 1248−56.
(56) Dobrynin, K.; Abdrakhmanova, A.; Richers, S.; Hunte, C.; Kerscher, S.; Brandt, U. Characterization of two different acyl carrier proteins in complex I from Yarrowia lipolytica. *Biochim. Biophys. Acta* **2010**, *1797* (2), 152−9.
(57) Staszczak, M. The role of the ubiquitin-proteasome system in the response of the ligninolytic fungus Trametes versicolor to nitrogen deprivation. *Fungal Genet Biol.* **2008**, *45* (3), 328−37.
(58) Swatek, A.; Staszczak, M. Effect of Ferulic Acid, a Phenolic Inducer of Fungal laccase, on 26S Proteasome Activities In Vitro. *Int. J. Mol. Sci.* **2020**, *21* (7), 2463 DOI: 10.3390/ijms21072463.
(59) Howell, L. A.; Peterson, A. K.; Tomko, R. J. Proteasome subunit alpha1 overexpression preferentially drives canonical proteasome biogenesis and enhances stress tolerance in yeast. *Sci. Rep.* **2019**, *9* (1), 12418.
(60) Ustrell, V.; Hoffman, L.; Pratt, G.; Rechsteiner, M. PA200, a nuclear proteasome activator involved in DNA repair. *EMBO J.* **2002**, *21* (13), 3516−25.
(61) Rodriguez-Iglesias, A.; Schmoll, M. Protein phosphatases regulate growth, development, cellulases and secondary metabolism in Trichoderma reesei. *Sci. Rep.* **2019**, *9* (1), 10995.
(62) De, S.; Muhlemann, O. A comprehensive coverage insurance for cells: revealing links between ribosome collisions, stress responses and mRNA surveillance. *RNA Biol.* **2022**, *19* (1), 609−621.
(63) Jamar, N. H.; Kritsiligkou, P.; Grant, C. M. Loss of mRNA surveillance pathways results in widespread protein aggregation. *Sci. Rep.* **2018**, *8* (1), 3894.
(64) Aggen, J. B.; Nairn, A. C.; Chamberlin, R. Regulation of protein phosphatase-1. *Chem. Biol.* **2000**, *7* (1), R13−23.
(65) Andrews, P. D.; Stark, M. J. R. Type 1 protein phosphatase is required for maintenance of cell wall integrity, morphogenesis and cell cycle progression in Saccharomyces cerevisiae. *J. Cell Sci.* **2000**, *113* (Pt 3), 507−20.
(66) Hu, K.; Li, W.; Wang, H.; Chen, K.; Wang, Y.; Sang, J. Shp1, a regulator of protein phosphatase 1 Glc7, has important roles in cell morphogenesis, cell cycle progression and DNA damage response in Candida albicans. *Fungal Genet Biol.* **2012**, *49* (6), 433−42.

(67) Cannon, J. F. Function of protein phosphatase-1, Glc7, in Saccharomyces cerevisiae. *Adv. Appl. Microbiol* **2010**, *73*, 27−59.
(68) Kervestin, S.; Li, C.; Buckingham, R.; Jacobson, A. Testing the faux-UTR model for NMD: analysis of Upf1p and Pab1p competition for binding to eRF3/Sup35p. *Biochimie* **2012**, *94* (7), 1560−71.
(69) Gonzalez, C. I.; Bhattacharya, A.; Wang, W.; Peltz, S. W. Nonsense-mediated mRNA decay in Saccharomyces cerevisiae. *Gene* **2001**, *274* (1−2), 15−25.
(70) Czaplinski, K.; Ruiz-Echevarria, M. J.; Paushkin, S. V.; Han, X.; Weng, Y.; Perlick, H. A.; Dietz, H. C.; Ter-Avanesyan, M. D.; Peltz, S. W. The surveillance complex interacts with the translation release factors to enhance termination and degrade aberrant mRNAs. *Genes Dev.* **1998**, *12* (11), 1665−77.
(71) Wang, W.; Czaplinski, K.; Rao, Y.; Peltz, S. W. The role of Upf proteins in modulating the translation read-through of nonsense-containing transcripts. *EMBO J.* **2001**, *20* (4), 880−90.
(72) Ivanov, P. V.; Gehring, N. H.; Kunz, J. B.; Hentze, M. W.; Kulozik, A. E. Interactions between UPF1, eRFs, PABP and the exon junction complex suggest an integrated model for mammalian NMD pathways. *EMBO J.* **2008**, *27* (5), 736−47.
(73) Zhang, Y.; Sachs, M. S. Control of mRNA Stability in Fungi by NMD, EJC and CBC Factors Through 3′UTR Introns. *Genetics* **2015**, *200* (4), 1133−48.
(74) Eisenberg, D.; Gill, H. S.; Pfluegl, G. M.; Rotstein, S. H. Structure-function relationships of glutamine synthetases. *Biochim. Biophys. Acta* **2000**, *1477* (1−2), 122−45.
(75) Zhu, J.; Song, S.; Sun, Z.; Lian, L.; Shi, L.; Ren, A.; Zhao, M. Regulation of glutamine synthetase activity by transcriptional and posttranslational modifications negatively influences ganoderic acid biosynthesis in Ganoderma lucidum. *Environ. Microbiol* **2021**, *23* (2), 1286−1297.
(76) Baidya, S.; Cary, J. W.; Grayburn, W. S.; Calvo, A. M. Role of nitric oxide and flavohemoglobin homolog genes in Aspergillus nidulans sexual development and mycotoxin production. *Appl. Environ. Microbiol.* **2011**, *77* (15), 5524−8.
(77) Wagner, D.; Wiemann, P.; Huss, K.; Brandt, U.; Fleissner, A.; Tudzynski, B. A sensing role of the glutamine synthetase in the nitrogen regulation network in Fusarium fujikuroi. *PLoS One* **2013**, *8* (11), No. e80740.
(78) Duellman, S. J.; Valley, M. P.; Kotraiah, V.; Vidugiriene, J.; Zhou, W. H.; Bernad, L.; Osterman, J.; Kimball, J. J.; Meisenheimer, P.; Cali, J. J. A bioluminescence assay for aldehyde dehydrogenase activity. *Anal. Biochem.* **2013**, *434* (2), 226−232.
(79) Shortall, K.; Djeghader, A.; Magner, E.; Soulimane, T., Insights into Aldehyde Dehydrogenase Enzymes: A Structural Perspective. *Front Mol. Biosci* **2021**, *8*.

https://doi.org/10.1021/acs.jafc.3c06083
J. Agric. Food Chem. 2024, 72, 1361−1375